FLOW PERFORMANCE COMPARISON ALONG THE CENTERLINE IN STRAIGHT AND S-SHAPED DIFFUSER

Amit Sharma[1], Arun Gupta[2], Hardial Singh[3,*]

ABSTRACT

In this paper of the S-shaped diffuser with area ratio (AR) 1.5, an experimental investigation was conducted to analyze the effect of the change in curvature of a straight-wall diffuser. During this study, a Straight diffuser was changed in to a curved diffuser at different angles as their same upper and lower limbs (60/60, 90/90). Profile equations of diffusers were generated with the help of MATLAB/Simulink v2017a software. In this work centerline length is constant for all three profiles, Centerline length that's utilized in the sector of circle and radius of curvature is calculated. S-shaped diffuser had a different unique angle with square inlet and a rectangular outlet. S-shaped diffuser C_{PR} and C_{TL} results compared with a straight walled diffuser with the different inlet velocity and Reynolds Number. These outcomes from this research obtained the coefficient of static pressure gain and coefficient of total pressure loss for the three profile of the diffuser (Straight, 60/60, and 90/90 S-Shaped Diffuser).

Keywords: Coefficient of Static Pressure Recovery, Coefficient of Total Pressure Loss, S-Shaped Diffuser

INTRODUCTION

A diffuser is a mechanical device which recuperates the pressure energy from the flowing fluid at the expense of its kinetic energy. The diffuser is of numerous kinds of namely axial, radial and curved depending on the geometry and design and finds very wide application in the field of aerospace and turbo-machinery. S-Shaped diffuser is finding huge applications in the field of aircraft applications due to space restrictions and design compatibility. S-Shaped diffusers are one of the popular types of curved diffusers. Generation of very strong pressure driven streamwise vortices due to the inflection in the curvature along the direction of flow makes in these diffusers very complicated. Since now, numerous analysts have been carried out on S-Shaped diffuser managing with the issue like impact of different inlet conditions, effect of angle of attack, effect of area ratio, effect of aspect ratio, effect of different inlet and outlet cross-section geometries, effect of angle of turn and many more on pressure recovery and non-uniformity of flow through it. The stream in these ducts becomes complicated because ofthe inflection in the curvature along the direction of flow and the generation of strong pressure drovestreamwise vortices. The stream attributes in these ducts are additionally by the inlet conditions and the radius of curvature.

Fox and Kline [1] examined the flow administrations of curved diffusers. They reasoned that stream administrations rely upon the proportion of Centerline sweep to throat width, turning point, and territory proportion. They have additionally reasoned that there was a fast drop off in passable zone proportion for the primary slow down point of confinement as the turning edge is expanded. The turning edge variety examined was 0 to 90 degree. R.W. Fox et al. [2] author did an investigation of curved diffusers and another investigation of factors in 2-D straight walled diffusers. It comes about, they built up a diagram of stream administrations for unstalled and slowed down curved diffuser for the stream to turn an edge of 0 to 90 degree with a distinction of 100 each. The geometry of turn/limb was a circular segment and straight zone appropriation typical to the inside line. Guo and Seddon [3, 4] studied the impact of whirlin S-formed diffusing diffuser utilized as a part of the present-day aerospace. They have proposed distinctive strategies for enhancing the result of executed work. Majumdar et al. [5] analyzed concentrated the flow in an S-formed diffusing pipe of rectangular cross-sectional and having area ratio 2. They found that vertical movements created in the pipe alter their course of revolution past the enunciation plane. The general Pressure recuperation/recovery is low when contrasted with straight diffuser and division stash was seeing at emphasis plane. Johnston [6] worked on the diffuser outline and execution examination of the basic diffuser with thin inlet limit layer

[1] Departmental of Mechanical Engineering, Govt. Engineering College of Bikaner, India
[2, 3] Department of Mechanical Engineering, Amity University Haryana, India
*E-mail address:hardialsingh3@gmail.com
Orcid id: orcid.org/ 0000-0003-0653-4807, 0000-0003-0215-7194, 0000-0001-9134-3428

and subsonic stream utilizing a computational work called the bound together indispensable strategy. The strategies give valuable outcomes including Pressure pick up, area of detachment and slowed down region and leave plane profile, which might be utilized to assess the Pressure loss and different stream twisting sign, The UIM (Universal Input Method) comes about were contrasted and RANS (Reynolds normal Navier Strokes) techniques and other ordinarily utilized CFD (Computational Fluid Dynamics) Codes and UIM Results were observed to be great and superior to another strategy.

K. Saha et al. [7] considered different cross-segment shapes on various inlets have been broke down utilizing standard turbulence demonstrates. For every one of the diffusers, the point of turn 22.50 the centreline length 300mm and the roundabout leave span 50 mm have been kept constant. Oval-mold inlet pipe blower displays the best exhibitions in terms of pressure repayment/profit, loss coefficient, and stream curved conditions on collision, while Square Conduit provides the most awesome stream trademark. Progression of inlet size for equality with the motor is one of the important issues in the S-size plan. Lienand Leschziner [8] are inconsistent that average stream facilities are expected in S-shaped diffusers, and unrest models are insensitive to the field, while unrest is very sensitive to the energy sector unrest model variations. Then ambika V. et al. [9] look and flow analysis of S-duct diffuser has been investigated, which is used directly in many jet craft hose systems so that less drag and engine conditions can be reduced compared to straight-wall diffuser design. They re-defined the position parameters of the radiation flow such as fixed pressure recovery and total pressure loss by adding a distorted generator. Geometry based on Fox and Kline on linear field-ratios to get out of the inlet. Design of diffuser built in *CATIA V5* and computational process on *ANSI Fluent* with MAC number value of 0.6 and 1.0 to boost static pressure recovery. The SVG pair was attached to each edge. A Jasmine et al. [10] an experimental and numerical investigation of flow management was examined in comparison to energy promoters and in an air intake S-shaped diffuser compared to energy. Turning angle 45/45 is used with Maintenance Area ratio 3. The simulation was done on *ANSYS-FLUENT ver.16.2* software. Performance experiment Reynolds number 5.8×10^4 and unrest contrast is 4.1%. The use of energy promoters reduces the outer surface boundary layer separation to a great extent, resulting in static pressure coefficient increase and total pressure decreases. Reichert and Wendt [11] used the fin-type vortex generator for secondary flow management and a respectable improvement is located in different flow parameters of the tube. Pradeep and Sulere [12], the Vortex generator uses the jet and receives a decrease of 20% in the total pressure loss and flow deformation coefficient within the diffuser. From the beginning of the 21st century, the investigation has shown a keen interest in design automation and improvement of S-ducts. Anand [13, 14] and rectangular (90/90 degree) diffuser region ratios 1.9 and 2.0 are different. Apart from this, important checks are done in the area of performance-improvement of S-duct by secondary flow control. Lefantzi and Knight [15] has developed an automatic design optimization technique for obstruction of taking S-duct such as airframe pressure, space, and engine-face line-of-sight barrier. However, these diffusers have been dependent on the effect of offset on the adverse effects and pressure recovery of the flow. Manoj K. Gopaliyaet.al. [16] have taken the impact of Offset on the S-size diffuser of 90°/90° turn with a rectangular inlet (aspect ratio 2) and half circle outlet with the regional ratio. In addition, the effect of the Reynolds number has been investigated by the author.

The present work contributes in this area of research providing the performed on the various inlet velocity and Reynolds number, to find out the pressure recovery coefficient and total pressure loss coefficient. The comparison has been made between a straight walled diffuser and S-Shaped diffuser with different turning angle (60deg. & 90deg.) to evaluate the overall performance of the diffuser.
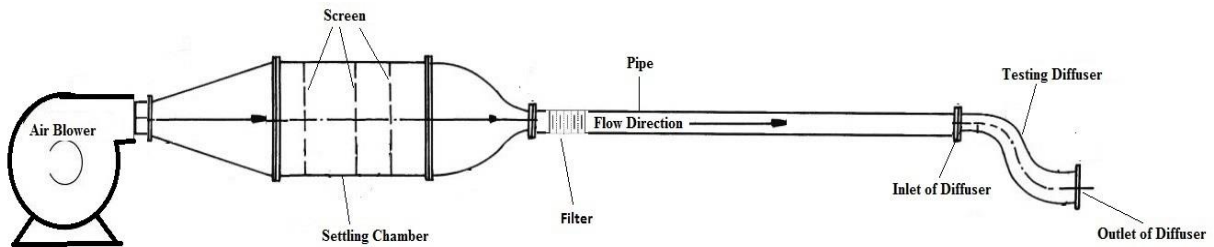
EXPERIMENTAL SETUP

The experimental setup was including measuring instruments like a Pitot tube for centerline velocity measurement, U-tube manometer for static pressure observation, and Air blower for making a stream of air in the test segment. Air blower has stream speed/velocity modification dial that is accustomed to performing the examination at a different speed and various Reynold's number. Settling Chamber and Filter were appended to accomplish and stabilizes the fluid stream.

A800W Blower was physically mounted on a stool with a speed adjustment dial. A 50 mm distance across pipe of length 4 m was connected with the blower. In between of these two, a settling chamber was attached for the

settling flow behavior and 3 single layer works were attached at the entrance of the pipe so concerning uniform and turbulence in the flow. The Pitot tube was introduced in the pipe near the inlet of the diffuser for measuring velocity at centerline utilizing total pressure and static pressure.

Two profiles are made utilizing with a similar area ratio of 1.5, constant centerline 500mm however straight walled and different turning angle 60/60 and 90/90 S-shaped individually were using in the experiment. Testing diffuser mounted into the testing setup and each one of the pressures tappings was connected to it. Pressure tapping was connected to the top and bottom surface of the diffuser taking the static pressure reading on the manometer. Each one of them is joined to U-tube manometer involving 22 U-tube Manometers altogether. These manometers are settled at a point of 45 degrees from the surface. An 8-layer mesh is appended toward the finish of the diffuser in order to restrict the entry of air from the atmosphere. There some central hole was present for total pressure measurement and a null point in a diffuser.

Air from the blower goes into the pipe and strikes the Pitot tube where centerline velocity was measured before going into the test diffuser. Each pressure tapping on the test diffuser is associated with the U-tube manometers keeping in mind the end goal to gauge the distinction in the pressure head. Every U-tube manometer has its one end connected to the pressure tapping of diffuser another end opens to the atmosphere and (manometric fluid upper position) H_2- (manometric fluid height down) H_1 is ascertained i.e. head difference. The block diagram of the experimental setup is shown in Figure -1.

Figure 1. Block diagram of experimental setup

Table 1. Parameters used in experimental calculation

Velocity(m/s)	Re	ρ_{air} (kg/m^3)	ρ_{water} (kg/m^3)	μ in Pa	sin45°
20.4	46240	1.2	1000	1.8e-5	0.71
26.6	60290	1.2	1000	1.8e-5	0.71

Instrument calibration is one of the primary processes used to maintain instrument accuracy. Calibration is a comparison between a known (standard) measurement instruments. Mass flow rate measurement is made at ten different values and then the average value is taken for further calculation. So, error in mass flow rate value is equal to $\pm2\%$, because by changing physical parameters like temperature etc. the uncertainty of a manometer reading is $\pm1/2$mm of the smallest scale graduation. This is due to the human eye's ability to interpolate between graduations.

## GEOMETRICAL AND EXPERIMENTAL DESCRIPTION

In this S-Shaped diffuser, different segments were set up with two different stream turn angles i.e. 60/60, and 90/90. Same turn angle was utilized as a part of both upper and lower arms. In 60/60 Section the sweep of ebb and flow at centerline for both upper and lower arms was 238 mm and with kept up area ratio 1.5 of the diffuser outlet. It has a square inlet and rectangular outlet of the diffuser. The width was comparably dispersed equally to the inside center line length of 500mm. The Sectioned S-Shaped diffuser was manufactured in six segments depends upon the turn angle and radius of curvature shown in figure-2. The examination was directed with air as the accompanying fluid in the test segment. Inlet velocity is estimation with the assistance of a pitot-static tube, which is arranged at some separation before the inlet area of the diffuser channel toward the fluid stream.

Table 2. Some parameter of experimental descriptions

S/No	Parameter	Value
1	Center length of Diffuser	500 mm
2	Area of Inlet Cross Section	1156 mm²
3	Area of Outlet Cross Section	1734 mm²
4	Area Ratio	1.5

Table 3.S-Shaped Diffuser Turning Angle with Radius of curvature

S/No.	Turning Angle (in degree)	The radius of Curvature (Rc) (mm)
1	60/60	238
2	90/90	159
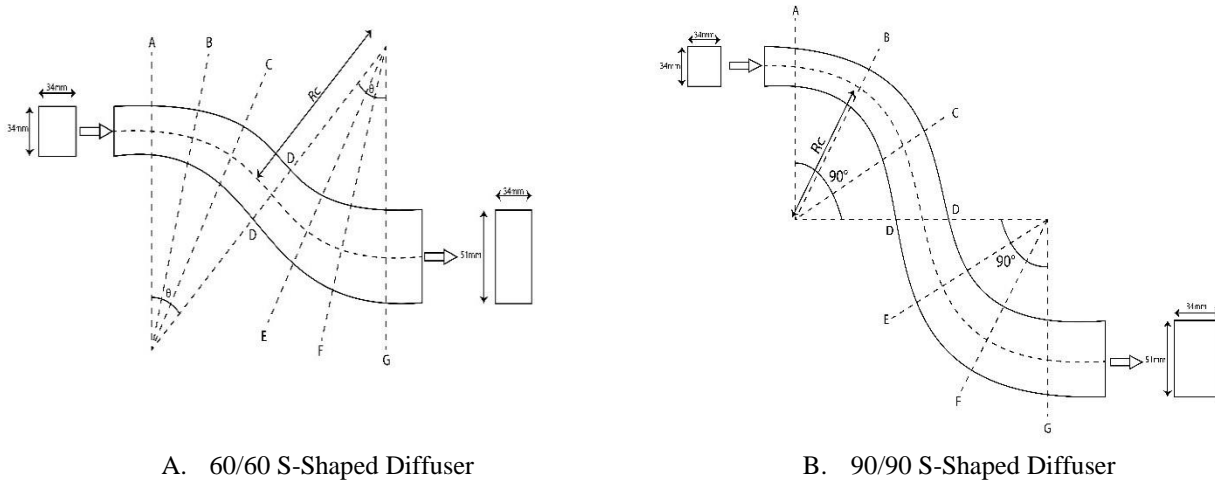
A. 60/60 S-Shaped Diffuser   B. 90/90 S-Shaped Diffuser

Figure 2. Schematic diagram of S-Shaped Diffuser

GOVERNING EQUATIONS

Governing equations for continuity and momentum, three-dimensional, steady state, Reynolds number, and Navier Stokes equations were numerically resolved, the unsteady flow of air was solved:

Continuity equation in coordinates (x, y, z)

$$\frac{\partial u}{\partial x} + \frac{\partial v}{\partial y} + \frac{\partial w}{\partial z} = 0 \tag{1}$$

X-Momentum equation:

$$u\frac{\partial u}{\partial x} + v\frac{\partial u}{\partial y} + w\frac{\partial u}{\partial z} = -\frac{1}{\rho}\frac{\partial P}{\partial x} + v\left[\frac{\partial^2 u}{\partial x^2} + \frac{\partial^2 u}{\partial y^2} + \frac{\partial^2 u}{\partial z^2}\right] + \frac{1}{\rho}\left[\left(\frac{\partial(-\rho\overline{u^2})}{\partial x}\right) + \partial\left(\frac{\partial(-\rho\overline{uv})}{\partial y}\right) + \left(\frac{\partial(-\rho\overline{uw})}{\partial z}\right)\right] \tag{2}$$

Y-Momentum equation:

$$u\frac{\partial v}{\partial x} + v\frac{\partial v}{\partial y} + w\frac{\partial v}{\partial z} = -\frac{1}{\rho}\frac{\partial P}{\partial y} + v\left[\frac{\partial^2 v}{\partial x^2} + \frac{\partial^2 v}{\partial y^2} + \frac{\partial^2 v}{\partial z^2}\right] + \frac{1}{\rho}\left[\left(\frac{\partial(-\rho\overline{uv})}{\partial x}\right) + \left(\frac{\partial(-\rho\overline{v^2})}{\partial y}\right) + \left(\frac{\partial(-\rho\overline{vw})}{\partial z}\right)\right] \tag{3}$$

Z-Momentum equation:

$$u\frac{\partial w}{\partial x} + v\frac{\partial w}{\partial y} + w\frac{\partial w}{\partial z} = -\frac{1}{\rho}\frac{\partial P}{\partial z} + v\left[\frac{\partial^2 w}{\partial x^2} + \frac{\partial^2 w}{\partial y^2} + \frac{\partial^2 w}{\partial z^2}\right] + \frac{1}{\rho}\left[\left(\frac{\partial(-\rho\overline{u'w'})}{\partial x}\right) + \left(\frac{\partial(-\rho\overline{v'w'})}{\partial y}\right) + \left(\frac{\partial(-\rho\overline{w'^2})}{\partial z}\right)\right] \quad (4)$$

PROFILE EQUATION GENERATION BY USING *MATLAB*

The profile conditions were produced with the assistance of MATLAB-2017a/Simulink programming shows in Figure 3. The conditions are utilized to depict the connection between x and y facilitates the profile manual for the stream. The conditions are created in bend fitting apparatus of MATLAB-2017a programming. The well-ordered process for creating the conditions introduced in this area.
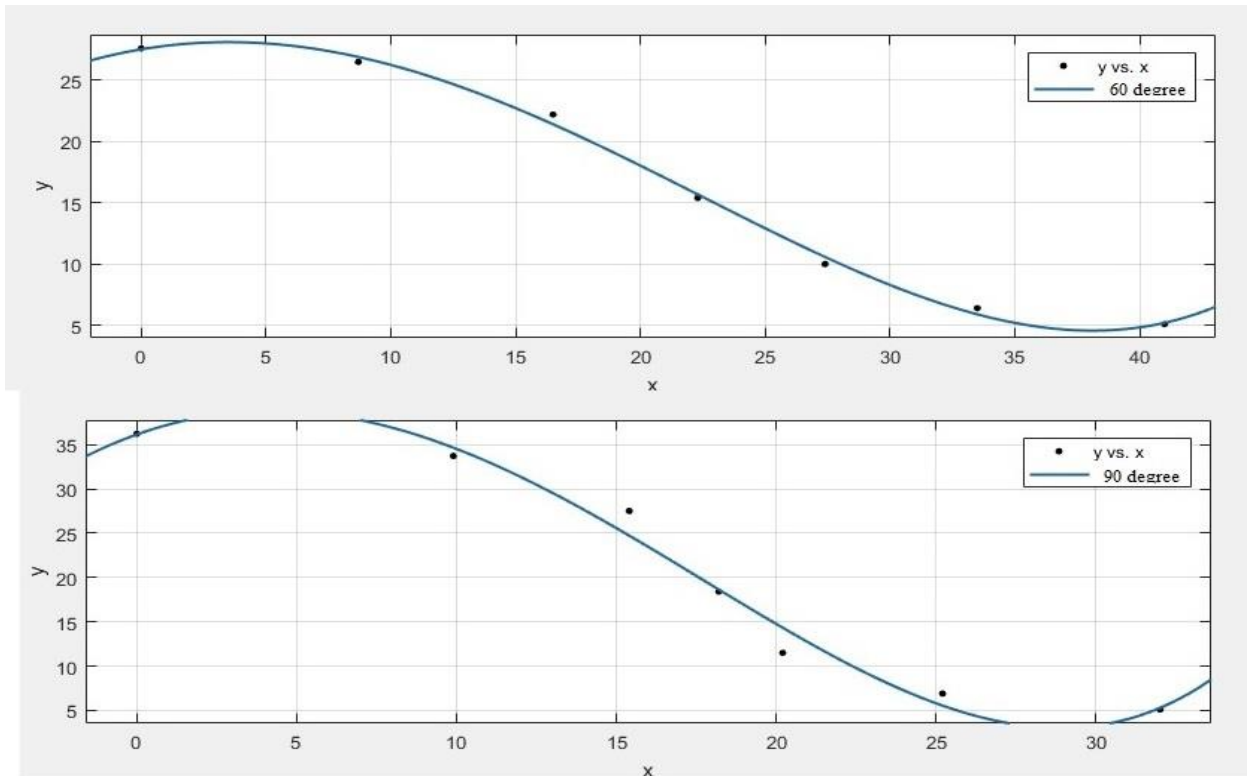

Figure 3. S-Shaped profile graphs of 60/60, and 90/90 plotted by *MATLABv2017a*

LINEAR MODEL 4TH DEGREE POLYNOMIAL 60/60 S-SHAPED DIFFUSER

$$f(x) = p_1 x^4 + p_2 x^3 + p_3 x^2 + p_4 x + p_5 \quad (5)$$

Coefficient (with 95% confidence bounds):
p_1 = 9.804e-06 (-7.449e-05, 9.41e-05)
p_2 = 0.0003183 (-0.006673, 0.00731)
p_3 = -0.05117 (-0.2351, 0.1327)
p_4 = 0.3429 (-1.274, 1.96)
p_5 = 27.53 (23.85, 31.2)
Goodness of fit:
SSE: 1.466
R-Square: 0.9972
Adjustment R-Square: 0.9917

RMSE: 0.8561

LINEAR MODEL 4TH DEGREE POLYNOMIAL 90/90 S-SHAPED DIFFUSER

$$f(x) = p_1 x^4 + p_2 x^3 + p_3 x^2 + p_4 x + p_5 \tag{6}$$

Coefficient (with 95% confidence bounds):
$p_1 = 5.668\text{e-}05\ (-0.001011, 0.001125)$
$p_2 = 0.001004\ (-0.06943, 0.07144)$
$p_3 = -0.1605\ (-1.635, 1.314)$
$p_4 = 1.283\ (-8.76.3, 11.33)$
$p_5 = 36.13\ (23.03, 49.23)$
Goodness of fit:
SSE: 18.55
R-Square: 0.981
Adjustment R-Square: 0.9429
RMSE: 3.046

PERFORMANCE PARAMETER
- **The coefficient of Static Pressure Recovery**

It shows that the magnitude by that kinetic energy has changed into pressure energy because of spreading action at any purpose location on the diffuser; it's shown by the equation [17]:

$$C_{PR} = \frac{P_s - P_{si}}{\frac{1}{2}\rho u^2} \tag{7}$$

where: - P_{si} – Inlet Static Pressure (Pa), P_s – Static Pressure (Pa), U – Avg. Inlet Velocity (m/s).

- **The coefficient of Total Pressure loss**

It is characterized by what quantity total pressure is lost a little of the mean recess dynamic pressure owing to viscous forces and turbulent intermixture.

A total pressure loss coefficient for a diffuser is outlined by the amendment in total pressure through the diffuser [17]:

$$C_{TL} = \frac{P_{ti} - P_t}{\frac{1}{2}\rho U^2} \tag{8}$$

where: - P_{ti} – Inlet Total Pressure (Pa), P_t – Total Pressure (Pa).

GRID INDEPENDENCY TEST

The grid independency test graph shown in figure4was performed to examine the difference in most extreme static pressure concerning the adjustment in the grid estimate. The extent of the element size lies between 0.9-1 mm and aggregate no of the element was 42,000. Quad/triangular cross-section was utilized with standard k-ε turbulence model. The maximum static pressure result obtained from the analysis was approximately close to the experimental results.

Table 4. Boundary conditions and fluid properties

Inlet boundary conditions:		
i	Types of Boundary	Velocity-inlet
ii	Reynolds Number	a) 46240 b) 60290
iii	Turbulence Intensity	5%
Outlet Boundary Condition:		
i	Types of Boundary	Pressure-outlet
ii	Pressure-specified	0 Pa (Gauge)
Wall Boundary Condition:		
i	Types of Boundary	Rough; 0.01mm Roughness height
ii	Shear Condition	No-Slip
Working Fluid Properties		
i	Working Fluid	Air
ii	The density of Working Fluid	1.225 kg/m^3
iii	Viscosity of working Fluid	1.78x10^{-5} kg/m-s
Element Shape		Quad/triangular
No of Cell		42000
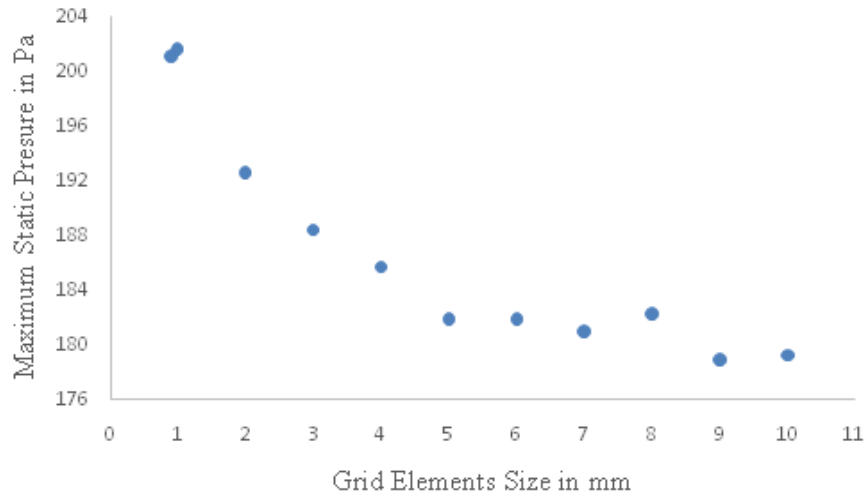
Figure 4. Grid independency test with a change in grid size

## RESULT AND DISCUSSION

The static pressure contours for the straight and S-Shaped diffuser has been shown in figure 5-10 at different inlet velocity of the operating fluid. In a straightdiffuser, the fluid stream in direct movement as guided by profile, another diffuser in this study has been a distinctive turning point so fluid guided by turned profile.

The static pressure contours for the S-Shaped diffuser with the various turning angle for exploratory inlet flow stream condition viz. Reynold number and inlet velocity are presented in figure 5-10. As it can be seen from assumes that coefficient of pressure gain is increased along the length. It is critical that with the adjustment in diverting point from 0 to 90 degree the stream redirects from the arched divider to curved divider. The processing of the stream brings a couple of flow misdistribution at the exit with the upper stream velocity externally of the curve.

In these figures, 5-6shows Straight walled diffuser flow uniform at the entrance however and non-uniform flow at the exit. Figure7-8 presents static pressure and velocity depict flow uniformity at the plane B and C plane, loss of uniformity and slight spatial property at the G plane and non-uniform flow at the exit attributable to secondarymotion along the convex/ concave wallbeyondthe inflectionplane. Figures 9-10shows static pressure and velocity depict flow uniformity at the plane C plane, loss of uniformity and slight asymmetry at the G plane and uniform and symmetrical flow at the exitattributable to secondarymotion along the convex/concave wallon the far
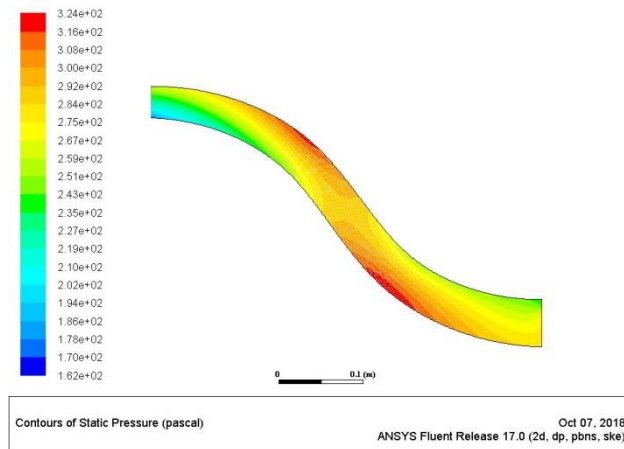
sidetheinflectionplane. At the plane D, flow ascertained that flow nature motion on the convex/concave in both the angle of the diffuser.
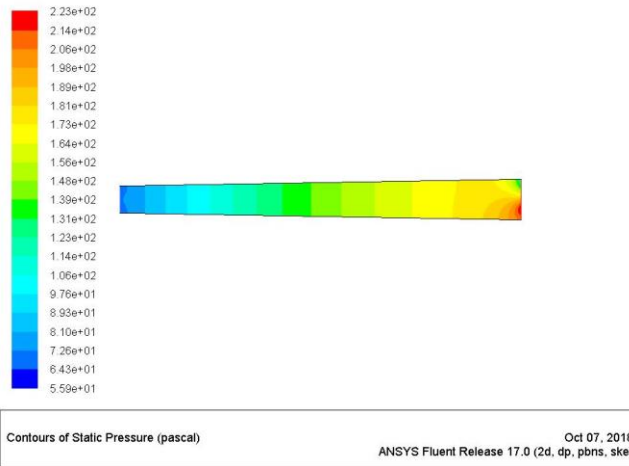
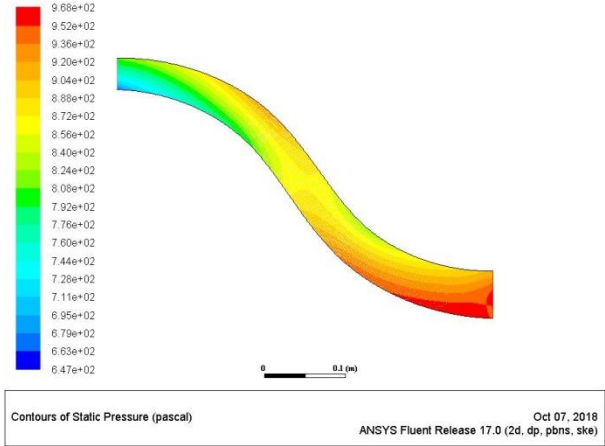**Figure 5**. Straight walled diffuser at 20.4 m/s
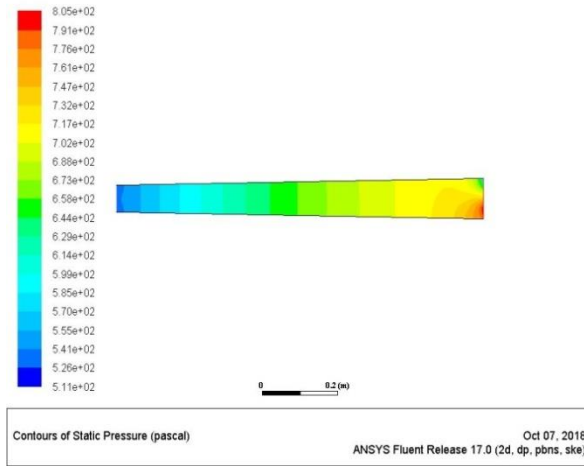
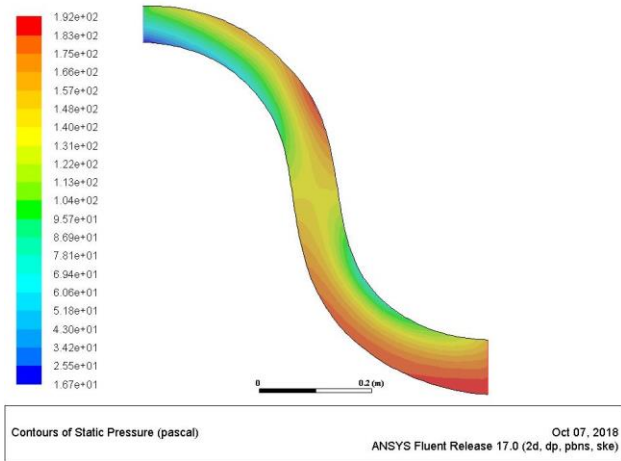**Figure 6**. Straight walled diffuser at 26.6 m/s

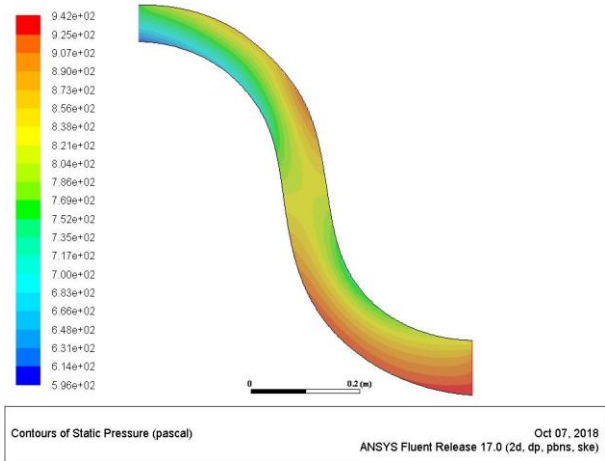**Figure 7**. 60/60 S-Shaped Diffuser at 20.4 m/s

Figure 8. 60/60 S-Shaped Diffuser at 26.6 m/s



Figure 9. 90/90 S-Shaped Diffuser at 20.4 m/s

**Figure 10**. 60/60 S-Shaped Diffuser at 26.6 m/s

Variation in Coefficient of Static Pressure Recovery (C_{pr}) Through The Length With Inlet Velocity 20.4 m/s and 26.6 m/s

Figure 11 shows the variant of the coefficient of static pressure recovery (C_{PR}) along the length of Straight walled and S-Shaped diffuser in figure11-12. The mass averaged flows that coefficient of static pressure

recovery value (C$_{PR}$) increases continuous in straight walled diffuser but 60/60, and 90/90 S-Shaped diffuser pressure recovery coefficient value increases only at the primary bend of the diffuser. Sudden decrease in the second turn recovery coefficient starts, due to the change in the direction of curvature, the plane is experienced as the initial turn, which leads to the turbulent mixture.
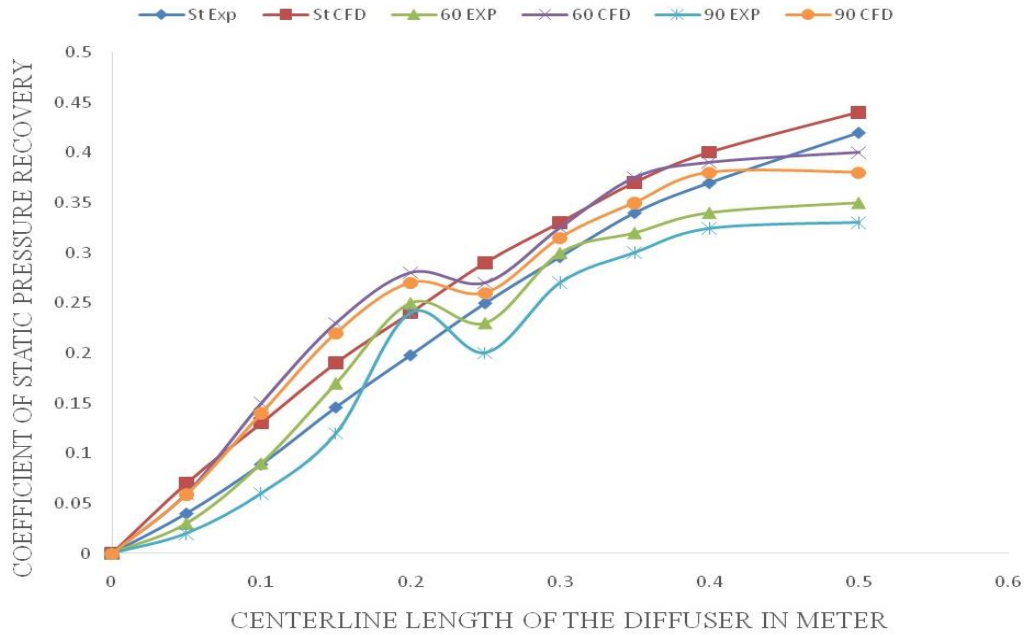
Figure 11. Variation of C$_{PR}$ along the length with Inlet velocity 20.6 m/s
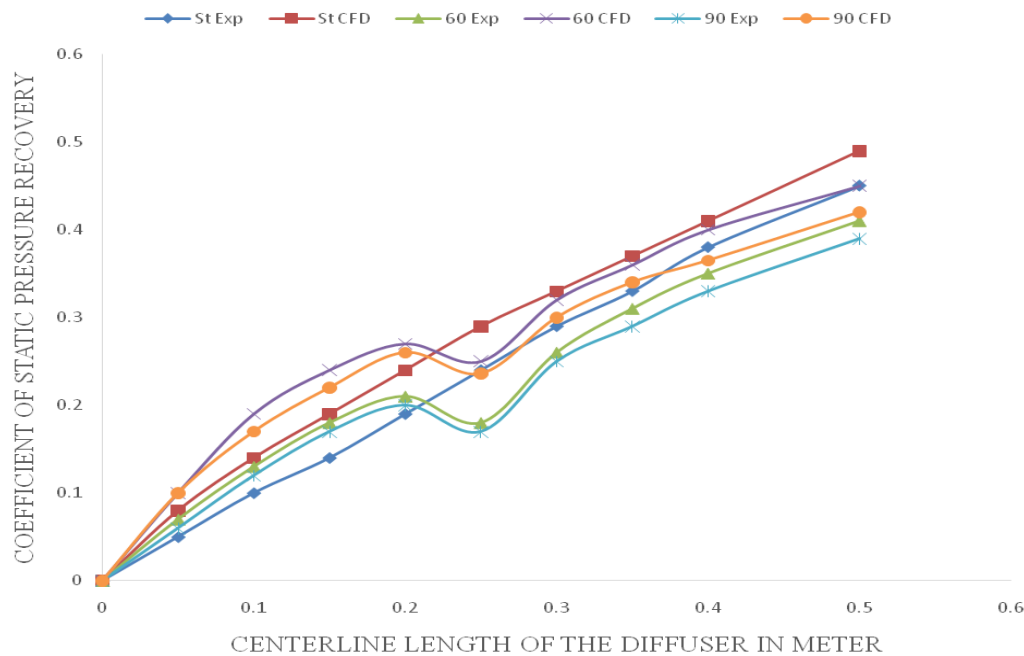
Figure 12. Variation of C$_{PR}$ along the length with Inlet velocity 26.6 m/s

Figure 11 represents the coefficient of static pressure recovery (C$_{PR}$) distributions along the length in the diffuser at various sections. The C$_{PR}$ values that were calculated experimentally by the test rig was increased in the initial phase up to plane B around 0.25m, after that its reduction due to flow separation until flow reattachment occurs somewhere before plane E at 0.3m and then it increases steadily till the plane's exit G. From now, in order to

obtain results a better understanding of the flow at the outlet. Straight walled diffuser and S-Shaped diffuser static pressure recovery coefficient increase continuously along the length. C_{PR} drops by 16.5% for 60/60 S-Shaped and C_{PR} drops 21.4% for 90/90 S-Shaped When compared to straight walled diffuser because of separation increase with turning angle. At the exit of the straight walled diffuser coefficient of pressure gain in experimental work is 0.42 but in simulation results 0.44, so we can observe the difference between the results at 4.72%. Similarly, in the 60/60-degreeexperimental and simulation results at the diffuser's outlet coefficient of pressure recovery is 0.35 and 0.40respectively. 90/90degree experimental and simulation results at the diffuser's outlet coefficient of pressure recovery are0.33 and 0.38 respectively.

Figure 12 represents the static pressure recovery coefficient distributions along the length within the diffuser at numerous sections. The C_{PR} values that were computed through an experiment by the test rig increased within the initial section up to plane B around 0.25m, after that it decreases due to flow separation until flow reattachment happens somewhere before plane E at 0.3m then it increases steadily until the exit plane G. Straight walled diffuser and S-Shaped diffuser static pressure recovery coefficient increase continuously along the length. C_{PR} drops by 8.9% for 60/60 S-Shaped and C_{PR} drops 13.3% for 90/90 S-Shaped When compared to straight walled diffuser because of separation increase with turning angle. The pressure recovery is lower, and the bending of the flow ends up in associate exit maldistribution with higher flow higher flow velocities on the outside of the bend. At the exit of the straight walled diffuser coefficient of pressure gain in experimental work is 0.45 but in simulation results 0.49, so we can observe the difference between the results at 8.9%. Similarly, in the 60/60-degree experimental and simulation results at the diffuser's outlet coefficient of pressure recovery is 0.41 and 0.45respectively. 90/90-degree experimental and simulation result at the diffuser's outlet coefficient of pressure recovery is 0.39 and 0.42 respectively. Figure 11-12 represents the coefficient of pressure recovery is increase as increasing the Reynolds number. It is easily observed that straight walled diffuser increment in the results at7.1%. In other diffuser were used in the experimental work 60/60 and 90/90-degree increment is 17% and 18.1% respectively.

Variation of Total Pressure Loss Coefficient (C_{tl}) Along the Length with Inlet Velocity 20.4 m/s and 26.6 m/s

The averaged mass flow impact on the entire pressure loss coefficient on the length of the diffuser is presented in figures13-14. Total pressure loss coefficient increased continuously in all diffuser however 60/60 and 90/90 S-Shaped diffuser fulminate pressure loss coefficient acquire initial bend and begin of the second bend. The second bend after the fluids tries to recover its lost energy and loss coefficient is nearly constant up to diffuser exit. At bend start that's introduce the centrifugal force in fluid motion. For all the Reynolds number the maximum C_{TL} is often for 90/90 S-Shaped diffuser. Within the graph at point 0.2m to the 0.3m coefficient of total pressure loss effects simply discovered thanks to the ever-changing flow moves on the convex/concave. For the experimental measurements, the trend of C_{TL} is almost like to the C_{TL} by computational.

Figure 13 represents the Total pressure loss along the length there is start at the turnthat effectively increases in losses as compared with other points of the diffuser. The graph represents at inlet condition losses are less but turning condition pressure loss high and then constant up. It can be further observed that average C_{TL} increase by 28.5% for 60/60 S-Shaped When compared to Straight walled diffuser because of turbulence and exchange of energy between streamline. Similarity average C_{TL} increases 42% for 90/90 S-Shaped when compared to the straight walled diffuser. The Resultanteffect of centrifugal force exists on the boundary layer of fluid.

Figure 14 represents the average C_{TL} increase by 33.3% for 60/60 S-Shaped and average C_{TL} increases 47.6% for 90/90 S-Shaped at Inlet velocity 26.6 m/s. When compared to Straight walled diffuser because the high-speed central velocity was driven to a concave part of diffuser wall and turbulence exchange of energy between streamline.Typically, reduction in C_{TL} as a result of a decrease in total pressure with diffuser and segregation area on the outer surface. The high-speed velocity was driven to a concave part of the diffuser wall and produces a complicated movement of flow. Generation of vortices inflowthat introduces the centrifugal force in the diffuser.
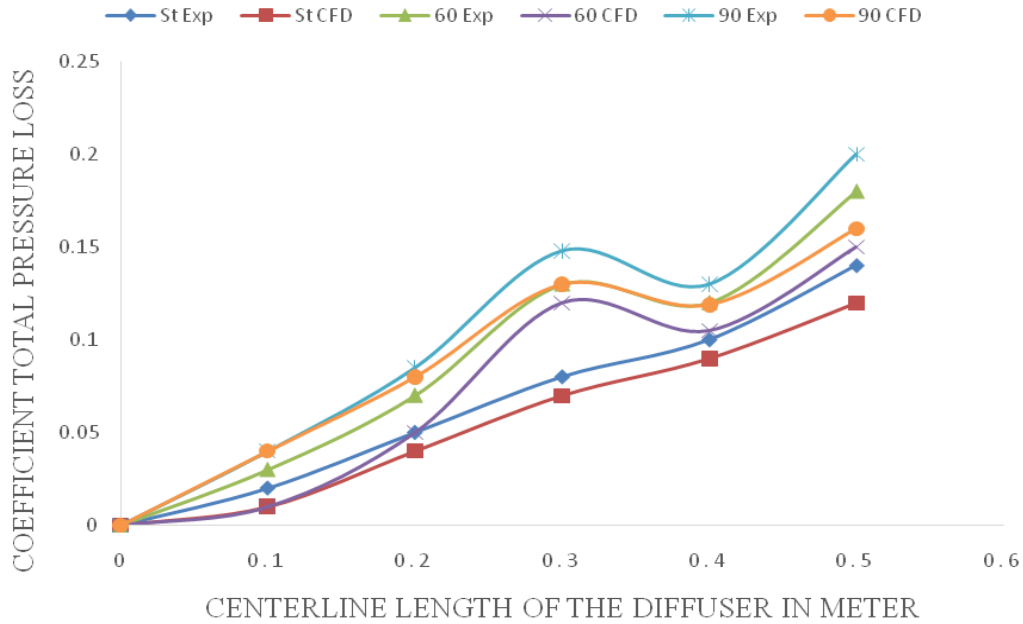
Figure 13. Variation of C_{TL} along the length with inlet velocity 20.6 m/s
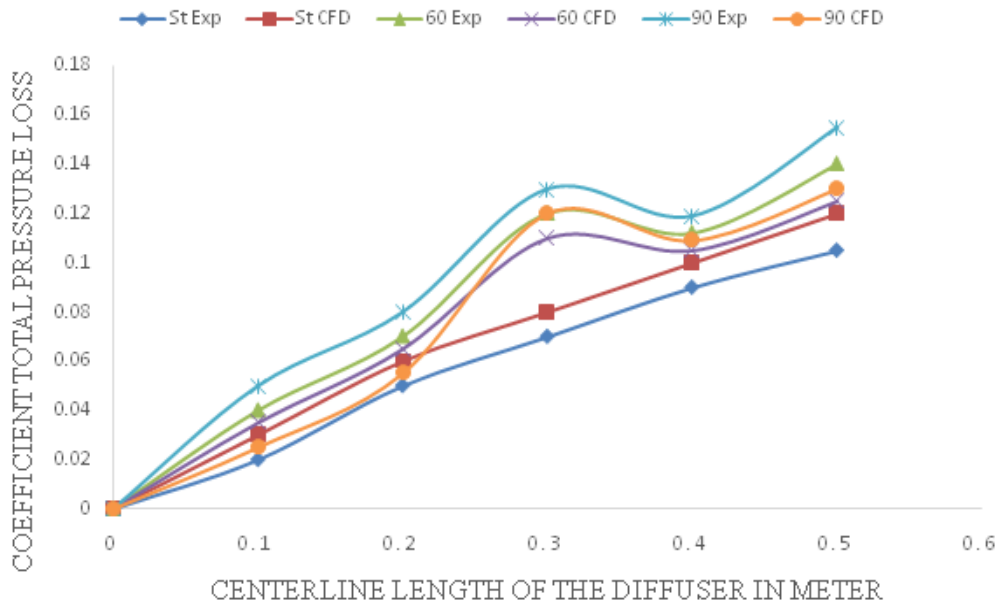
Figure 14. Variation of C_{TL} along the length with inlet velocity 26.6 m/s

VALIDATION OF EXPERIMENTAL AND COMPUTATIONAL RESULTS

A preliminary investigation has been performed in experimental work to validate the computational results in all three diffuser profiles. The comparison between the experimental and computational process for std k-ε model static pressure recovery coefficient results at outlet condition are shown in table 3. The std k-ε model computational C_{PR} at the outlet is close to experimental C_{PR}. The loss coefficient values are also close to both experimental and computational.

Table 5.Comparison of Experimental and CFD results in Straight walled and 60/60 S-Shaped Diffuser

Reynolds No.	Straight Exp. C_{PR}	Straight CFD C_{PR}	Error %	60/60 Exp. C_{PR}	60/60 CFD C_{PR}	Error in %
46240	0.42	0.44	4.5	0.35	0.40	14.2
60290	0.45	0.49	8.1	0.41	0.45	9.7

CONCLUSION

The experimental and computational investigation has been conducted on the straight and S-Shaped diffuser of 60/60 and 90/90-degree diffuser. The following conclusion was drawn from the present examination:

- The wall static pressure distribution demonstrates that the procedure of diffusion along the convex/concave wall is essentially higher than that of the concave/convex wall.
- Increase in Reynolds number leads to an increase in the coefficient of static pressure gain and also decrease in coefficient of total pressure loss at all the reading stations along the center line of the diffuser.
- The loss of uniformity in the flow along the center line of the diffuser at the outlet.
- Generation of counter-rotating vortices can be attributed to centrifugal forces.
- Flow separation region especially on the outer surface of the diffuser.
- 60/60-degree gave the 5.25% which is better performance comparison in the 90/90-degree.
- The Straight walled diffuser gave a better result when compared to both S-shaped Diffuser (60/60, and 90/90 S-Shaped Diffuser).

NOMENCLATURE

AR	Area Ratio
A_1	Area of Inlet Section (m^2)
W_1	Width of Inlet (m)
AS	Aspect Ratio
W	Width (m)
ε	Rate of turbulent kinetic energy dissipation (J/kg.s)
P	Pressure (Pa)
Psi	Static Pressure at inlet (Pa)
Ps	Static Pressure (Pa)
C_{PR}	Coefficient of Static Pressure Recovery
C_{Pi}	Coefficient of Static Pressure Recovery ideally
SSE	Sum of Squares due to error
Re	Reynolds Number
	$Re = \rho\, U_{avgi} D_h / \mu$
A_2	Area of Outlet Section (m^2)
W_2	Width of Outlet (m)
ρ	Density of Fluid (Kg/m^3)
U_{avgi}	Mass average mean velocity at inlet
μ	Viscosity of Working Fluid (Pa.s)
D_h	Hydraulic Diameter at the inlet
	$D_h = 4Area/Perimeter$ (m)
Pti	Total pressure at inlet (Pa)
Pt	Total pressure (Pa)
C_{TL}	Coefficient of Total Pressure Loss
v	Velocity of Fluid (m/s)
RMSE	Root mean squared error

REFERENCES

[1]. Kline, S. J. Optimum design of straight-walled diffusers. Trans. ASME. (1959); Ser. D: 81(3): 321-331.

[2]. Fox RW, Kline SJ. Flow regimes in curved subsonic diffusers. Journal of Basic Engineering. 1962 Sep 1; 84(3):303-12.

[3]. Guo RW, Seddon J. The swirl in an S-duct of typical air intake proportions. The Aeronautical Quarterly. 1983 May;34(2):99-129.

[4]. Guo RW, Seddon J. Swirl characteristics of an S-shaped air intake with both horizontal and vertical offsets. The Aeronautical Quarterly. 1983 May;34(2):130-46.

[5]. Majumdar B, Mohan R, Singh SN, Agrawal DP. Experimental study of flow in a high aspect ratio 90 deg curved diffuser.1998:83-89.

[6]. Johnston J, Johnston J. Diffuser design and performance analysis by unified integral methods. In33rd Joint Propulsion Conference and Exhibit 1998 Mar 1 (p. 2733).

[7]. Saha K, Singh SN, Seshadri V, Mukhopadhyay S. Computational analysis on flow through transition S-diffusers: Effect of inlet shape. Journal of aircraft. 2007 Jan; 44(1):187-93.

[8]. Lien FS, Leschziner MA. Computational modelling of 3D turbulent flow in S-diffuser and transition ducts. InEngineering Turbulence Modelling and Experiments 1993 Jan 1 (pp. 217-228). Elsevier.

[9]. Thenambika, V., Ponsankar, S., & Prabhu, M. K. Design and flow analysis of S duct diffuser with submerged vortex Generators. International Journal of Engineering Research and Applications. 2016; 6(2): 79-84.

[10]. Jessam RA, Al-Kayiem HH, Nasif MS. Flow control in s-shaped air intake diffuser of gas turbine using proposed energy promoters. InMATEC Web of Conferences 2017 (Vol. 131, p. 02006). EDP Sciences.

[11]. Reichert BR, Wendt BR. Improving diffusing S-duct performance by secondary flow control. In32nd Aerospace Sciences Meeting and Exhibit 1994 Feb 1 (p. 365).

[12]. Pradeep AM, Sullerey RK. Secondary flow control in a circular S-duct diffuser using vortex generator jets. In2nd AIAA Flow Control Conference 2004 (p. 2615).

[13]. Anand, R. B., Rai, L., Singh, S. N. Flow and performance characteristics of 22.5 º/22.5 º S-Shaped circular diffuser. In Proc. of 28th National conference on FMEP Chandigarh, India. 2001.

[14]. Anand RB, Rai L, Singh SN, Sharma OP. Flow characteristics of a low aspect ratio 90 deg/90 deg S-shaped diffuser. Journal of the Aeronautical Society of India. 2001 Nov; 53(4):239-52.

[15]. Lefantzi S, Knight DD. Automated design optimization of a three-dimensional S-shaped subsonic diffuser. Journal of Propulsion and Power. 2002 Jul; 18(4):913-21.

[16]. Gopaliya MK, Kumar M, Kumar S, Gopaliya SM. Analysis of performance characteristics of S-shaped diffuser with offset. Aerospace Science and Technology. 2007 Mar 1; 11(2-3):130-5.

[17]. Gopaliya MK, Jain P, Kumar S, Yadav V, Singh S. Performance improvement of s-shaped diffuser using momentum imparting technique. Journal of Mechanical and Civil Engineering. 2014 Mar; 11(3):23-31.